

Ameliorative Effects of Geraniol on Cyclophosphamide-Induced Nephrotoxicity: Evidence from Nuclear Factor Erythroid 2-related Factor 2 (Nrf-2) Activation and Apoptosis Modulation

Halime Tuba Canbaz¹, Mehmet Enes Sozen², Furkan Adem Canbaz³, Gokhan Cuce⁴, Serpil Kalkan⁴

¹Department of Histology and Embryology, University of Health Sciences, Hamidiye Faculty of Medicine, İstanbul, Türkiye; ²Department of Histology and Embryology, Alanya Alaaddin Keykubat University, Faculty of Medicine, Antalya, Türkiye; ³Department of Pediatric Urology, Sancaktepe Sehit Prof. Dr. Ilhan Varank Training and Research Hospital, İstanbul, Türkiye; ⁴Department of Histology and Embryology, Necmettin Erbakan University, Faculty of Medicine, Konya, Türkiye

Abstract:

Objective: The cyclophosphamide (CP)-related nephrotoxicity may impede cancer treatment. This study investigated the efficacy of geraniol (Ge) at two doses against CP nephrotoxicity.

Methods: Forty-two Wistar albino rats were allocated into six groups (n=7 each group): Group I, control; Group II, CP; Group III, CP+Ge 100 mg/kg; Group IV, CP+Ge 200 mg/kg; Group V, Ge 100 mg/kg; and Group VI, Ge 200 mg/kg. At the end of study, alterations in renal tissues were evaluated using hematoxylin-eosin and histopathological scores were determined. Masson's trichrome and Periodic acid-Schiff (PAS) staining were also performed for evaluation of fibrosis, parietal layer of Bowman capsule, and Bowman's space. Immunofluorescence analysis assessed oxidative stress and apoptosis. Consequently, the expression levels of nuclear factor erythroid 2-related factor 2 (Nrf-2), caspase 3, and caspase 9 were evaluated.

Results: CP caused the histopathological changes, including tubular damage, glomerular degeneration, interstitial inflammation. Ge restored the increased histopathological scores, parietal layer of Bowman capsule, and Bowman's space caused by CP without dose dependence (P<0.001 for both dose). CP decreased the expression of Nrf-2, while Ge improved this disturbance with greater efficacy at a higher dose (P<0.001 for all). CP exposure increased both caspase 3 and caspase 9 (P<0.001 for both). Ge decreased the expressions of caspase 3 and caspase 9 at two doses (P<0.001 for all). In addition, Ge was more effective in repairing caspase 3 at a higher dose (P=0.006).

Conclusion: Ge seems to effectively reverse CP-induced nephrotoxicity. The histopathological improvements are mediated by mechanisms involving the attenuation of oxidative stress and apoptosis. The efficacy of Ge is also dose-dependent.

Keywords: Apoptosis, Cyclophosphamide, Geraniol, Nephrotoxicity, Oxidative Stress

Submitted: April 28, 2026 Accepted: May 31, 2026 Published Online: June 20, 2026

How to cite this article: Canbaz HT, Sozen ME, Canbaz FA, Cuce G, Kalkan S. Ameliorative Effects of Geraniol on Cyclophosphamide-Induced Nephrotoxicity: Evidence from Nuclear Factor Erythroid 2-related Factor 2 (Nrf-2) Activation and Apoptosis Modulation. *Eur Res J.* 2026;12(8):867-875. doi: [10.18621/eurj.1306](https://doi.org/10.18621/eurj.1306)

Corresponding author: Halime Tuba Canbaz, MD., Assist. Prof., Phone: +90 216 777 82 60, E-mail: halimetuba.canbaz@sbu.edu.tr

This is an open-access article distributed under the terms of a Creative Commons Attribution-NonCommercial-NoDerivatives 4.0 International License, which permits any non-commercial use, sharing, distribution and reproduction in any medium or format, as long as you give appropriate credit to the original author(s) and the source, provide a link to the Creative Commons licence, and indicate if you modified the licensed material. You do not have permission under this licence to share adapted material derived from this article or parts of it.

Available Online at <https://www.eurj.org.tr>



Chemotherapeutic agents are being utilized more extensively owing to the rising prevalence of cancer. A notable adverse effect of anticancer medications is nephrotoxicity [1]. Tubular damage and acute renal injury result in significant morbidity and may necessitate the cessation of therapy. Consequently, attempts to avert nephrotoxicity induced by chemotherapeutic drugs hold significant clinical relevance [2].

Oxidative stress and elevated reactive oxygen species are the primary processes behind nephrotoxicity. Lipid peroxidation, DNA damage, and mitochondrial dysfunction contribute to renal impairment [3, 4]. The nuclear factor erythroid 2-related factor 2 (Nrf-2), a crucial regulator of the cellular antioxidant response, enhances the expression of antioxidant genes in response to oxidative stress [5]. The activation of Nrf-2 is the principal adaptive mechanism that safeguards cells against oxidative stress. Oxidative stress triggers apoptotic changes as well as the Nrf-2 pathway.

Oxidative stress induces cellular apoptosis by increasing the expression of the apoptotic proteins caspase 3 and caspase 9 [6]. Elevated production of caspase 3 and caspase 9 provides evidence at the tissue level that cellular damage transpires through apoptosis.

The processes discussed highlight the significance of antioxidants in mitigating damage associated with oxidative stress and apoptosis [7]. Geraniol (Ge), a monoterpene included in essential oils, has been identified for its anti-inflammatory, anticancer, and antioxidant properties. Although the preventive effects of Ge have been studied in many animal models of organ damage, there are few data about its efficacy in nephrotoxicity induced by various chemotherapeutic agents [8, 9]. The natural origin and comparatively low toxicity of Ge render it an attractive choice for supportive therapy. These properties may enhance its potential use in preventing organ toxicity associated with chemotherapy.

This study investigated the possible protective benefits of Ge in a histopathological model of nephrotoxicity produced by cyclophosphamide (CP). Ge was administered at two distinct dosages to assess dose-dependent effectiveness. Additionally, the investigation assessed whether this impact was mediated through the Nrf-2 pathway and the production of caspase 3 and caspase 9.

METHODS

The Animal Experiments Local Ethics Committee of Necmettin Erbakan University approved of this study (decision date: December 22, 2017; decision number: 2017-039). This study was conducted in accordance with institutional guidelines and international standards for the care and utilization of laboratory animals.

Animals and Experimental Design

A total of 42 male Wistar Albino rats were obtained from the institutional experimental medicine application and research center. They were 4 months old and weighing between 250 and 300 grams. The rats were given a standard diet and provided with tap water. The study was conducted under controlled environmental conditions of $22\pm 2^{\circ}\text{C}$ room temperature, 60% humidity, and a 12-hour light/dark cycle.

Six groups were randomly formed:

- Group I, (control group) with no procedure.
- Group II, (CP group), only CP was administered.
- Group III, (CP + Ge 100), CP and Ge (100 mg/kg) were administered.
- Group IV, (CP + Ge 200), CP along with Ge (200 mg/kg) were administered.
- Group V, (Ge 100), only Ge (100 mg/kg) was administered.
- Group VI, (Ge 200), only Ge (200 mg/kg) was administered.

Ge (Sigma Aldrich, 163333) was administered daily for a duration of 14 days. From days 8 to 14, CP (Endoxan, 500 mg IV solution prepared for infusion) at a dose of 20 mg/kg was provided daily. Ge was supplied via oral gavage, whereas CP was delivered via intraperitoneal injection. The doses and delivery methods for CP and Ge were established based on the literature [10, 11].

The experiment lasted 14 days. At the conclusion of the experimental period, anesthesia was induced by intraperitoneal injection of xylazine and ketamine. The dosages of the anesthetic drugs were 10 mg/kg and 90 mg/kg, respectively. Euthanasia was conducted via cervical dislocation under anesthesia; the kidneys of the experimental animals were removed and immersed in 10% neutral formaldehyde.

Histopathological Evaluation

Following 48 hours of fixation, the fixed tissues underwent dehydration through a sequence of increasing alcohol concentrations, were cleaned with xylene, and subsequently embedded in paraffin blocks. Sections of 3-5 μm in thickness were obtained from the paraffin blocks with a Microm HM325 rotating microtome. Tissue sections—three per slide—were prepared following mounting and labeling. The slices underwent standard hematoxylin and eosin (H&E) staining to assess the kidney architecture. Five criteria, including vacuolar degeneration, congestion, tubular dilatation, desquamation, and inflammatory cell infiltration, were evaluated. Histopathological scoring of each criterion was determined by evaluating these changes: absence (0), mild (1), moderate (2), severe (3) [12, 13]. The mean value of these five criteria composed a histopathological score per animal. Masson’s trichrome staining was also performed to evaluate the observational collagen deposition and fibrosis. ChemBio staining kit CB6095.0100 was used according to the manufacturer's instructions. Periodic acid–Schiff (PAS) staining was conducted to evaluate the parietal layer of Bowman’s capsule and Bowman's space; slices were stained with PAS for 5 minutes, during which the periodic acid interacted with the carbohydrates in the tissue, resulting in a purple-magenta coloration over 10 minutes using Schiff reagent. All histopathological assessments were performed blinded using a Zeiss Lab A1 light microscope.

Immunofluorescence Assessment

Paraffin sections underwent deparaffinization and rehydration. Antigen retrieval was accomplished by heating in a citrate buffer (10 mM, pH 6.0). To suppress endogenous peroxidase activity, 3% hydrogen peroxide (H₂O₂) was administered to the tissues. Super Block was administered for 30 minutes. The slides were treated overnight at +4°C with Anti-NRF2 Rabbit polyclonal antibody (1/1000; GB113808, Servicebio), ABclonal Caspase-3 Rabbit pAb (1/200, A2156), and ABclonal Caspase-9 Rabbit pAb (1/100, A2636). The next day, a secondary antibody, Goat Anti-Rabbit IgG H&L (1/500; Alexa Fluor® 488, ab150077) was applied for one hour at ambient temperature. Following a 30-minute wash with phosphate-buffered saline (PBS), the sections were incubated in a solution comprising PBS, glycerin, and Hoechst 33342 (ThermoFisher Scientific) and examined using a Zeiss Axio microscope (AxioCam 212 color camera). The mean intensity value was recorded using Zeiss software ZEN 3.12 (Zen lite).

Statistical Analysis

The statistical analysis was conducted using GraphPad Prism version 8.4.2. The Shapiro-Wilk test was done to assess the normality of numerical data. The Kruskal-Wallis test and post hoc Dunn’s test were conducted for the numerical variables that do not have a normal distribution. The variance of homogeneity was examined for normally distributed variables using

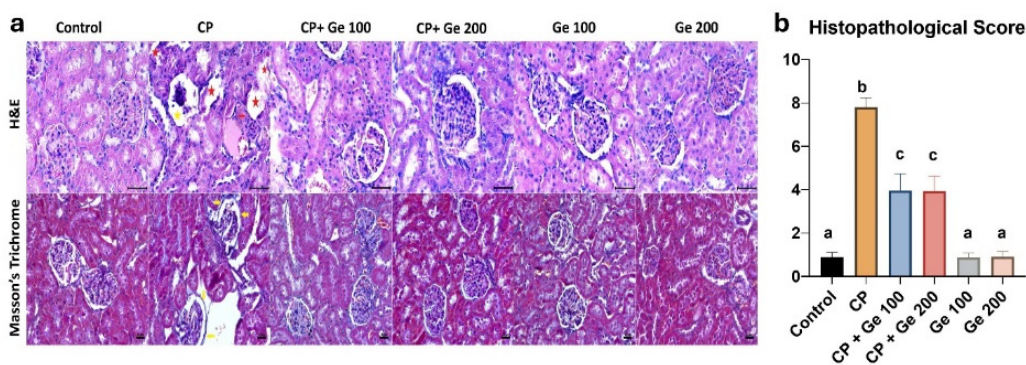


FIGURE 1. The findings of H&E and Masson's Trichrome staining. (a) Red star, tubular degeneration; yellow stars, dilated Bowman space (due to glomerular degeneration); red arrow, inflammation. Bars show 50 μm in H&E staining (×400). Yellow arrows show thickened Bowman's parietal capsule. Bars show 20 μm in Masson's Trichrome staining (×200). (b) Histopathological scores of the experimental groups based on five criteria evaluated using H&E staining. There is statistically significant difference between the groups not sharing the same letter (P<0.05). CP, Cyclophosphamide; Ge, Geraniol.

the Brown-Forsythe test. One-way ANOVA or Welch ANOVA was conducted based on the homogeneity of variance, utilizing Tukey or Dunnett T3 tests as post hoc analyses, respectively.

RESULTS

Histopathological Findings

The CP administration led to histopathological alterations, including tubular damage (vacuolization, degeneration, and dilation), glomerular degeneration, irregularities of Bowman's space, and interstitial inflammation. Masson's trichrome assessment also demonstrated increased interstitial collagen deposition, indicative of renal fibrosis, in the CP exposure. The Ge treatment was found to be effective in restoring these disturbances (Figure 1.a). The mean histopathological score of the CP group was elevated in comparison to the control (7.81 ± 0.43 vs. 0.88 ± 0.23 , $P < 0.001$). Ge at both dosages reduced the mean histopathological score in comparison to the CP group ($P < 0.001$ for both). The mean histopathological scores of CP+Ge 100 and CP+Ge 200 were similar (3.95 ± 0.78 and 3.93 ± 0.69 , respectively, $P > 0.05$). Figure 1.b demonstrates the histopathological scores among groups. PAS staining showed that the parietal layer of Bowman's capsule and Bowman's space were increased in CP exposure compared to the control ($P < 0.001$ for both). Ge, at both doses, reversed these

parameters (the parietal layer thickness and Bowman's space), which were increased with CP exposure ($P < 0.001$ for all). Based on PAS staining findings, both doses of Ge had similar efficacy ($P > 0.05$). Table 1 presents the numerical values of histopathological scores, the parietal layer of Bowman's capsule, and Bowman's space.

Immunofluorescence Assessment

The expression of Nrf-2 reduced in the CP group compared to the control group ($P < 0.001$). Both doses of Ge enhanced this reduction ($P < 0.001$ for both). In CP exposure, Ge demonstrated greater efficacy at a dose of 200 mg/kg as compared with 100 mg/kg ($P < 0.001$). The average intensity value of Nrf-2 in the CP group was 13.12 ± 1.42 , whereas it was 33.91 ± 1.40 in the control group. The Nrf-2 expression levels for CP+Ge at 100 mg/kg and CP+Ge 200 mg/kg were 29.62 ± 1.30 and 35.17 ± 2.21 , respectively (Table 1). Figure 2 depicts the immunofluorescence staining of Nrf-2 expression and graphs of the mean intensity values for the groups.

The expressions of both caspase 3 and caspase 9 were significantly elevated in the CP group (39.46 ± 1.07 and 34.10 ± 0.88 , respectively) compared with the control (14.45 ± 0.33 and 15.11 ± 0.72 , respectively) ($P < 0.001$ for both). Ge at both doses reduced the expression of apoptotic markers including caspase 3 and caspase 9 which were increased by CP

TABLE 1. Histopathological Scores, Immunofluorescence Expression Levels, and PAS Staining Parameters in Experimental Groups

	Histopathological score	Nrf-2 expression	Caspase 3	Caspase 9	Parietal layer (micrometer)	Bowman's space (micrometer)
Control	0.88 ± 0.23^a	$33.91 \pm 1.40^{a,d}$	14.45 ± 0.33^a	15.11 ± 0.72^a	1.505 ± 0.040^a	5.531 ± 0.259^a
CP	7.81 ± 0.43^b	13.12 ± 1.42^b	39.46 ± 1.07^b	34.10 ± 0.88^b	4.176 ± 0.516^b	9.357 ± 0.899^b
CP+Ge 100 mg/kg	3.95 ± 0.78^c	29.62 ± 1.30^c	25.46 ± 1.03^c	25.07 ± 0.89^c	2.057 ± 0.202^c	6.504 ± 0.693^c
CP+Ge 200 mg/kg	3.93 ± 0.69^c	35.17 ± 2.21^d	23.21 ± 1.86^d	25.43 ± 0.98^c	1.907 ± 0.097^c	7.016 ± 0.276^c
Ge 100 mg/kg	0.86 ± 0.22^a	$33.08 \pm 0.91^{a,d}$	15.23 ± 1.11^a	15.49 ± 0.07^a	1.814 ± 0.094^c	6.938 ± 0.275^c
Ge 200 mg/kg	0.91 ± 0.25^a	$31.63 \pm 1.44^{a,c}$	15.94 ± 0.40^a	15.52 ± 0.09^a	1.794 ± 0.106^c	$6.318 \pm 0.426^{a,c}$

Data are shown as mean \pm standard deviation. CP, Cyclophosphamide; Ge, Geraniol; Nrf-2, nuclear factor erythroid 2-related factor 2; PAS, Periodic acid-Schiff.

The different superscript letters demonstrate statistically significant difference between the groups ($P < 0.05$).

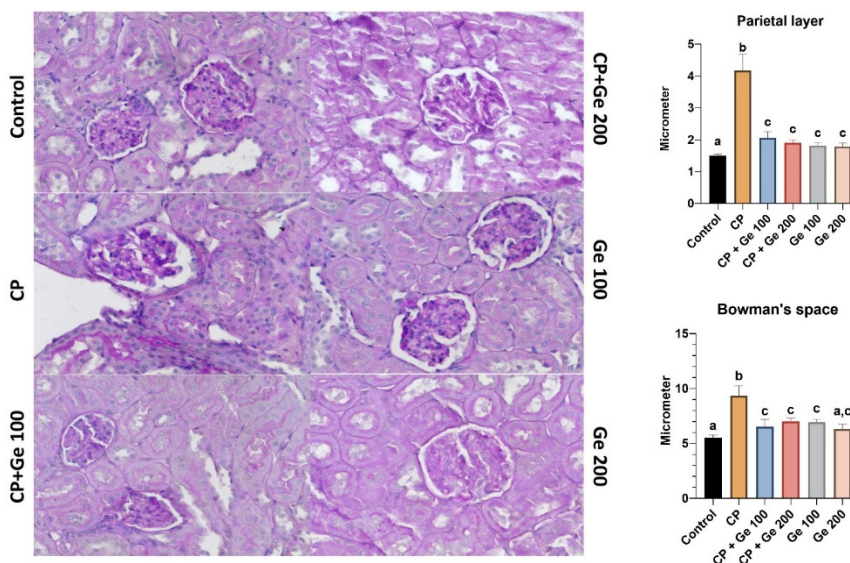


FIGURE 2. (a) PAS staining (Magnification ×400). (b) Graphical representation of the histomorphometric analysis of the parietal layer of Bowman's capsule and Bowman's space among groups. CP, Cyclophosphamide; Ge, Geraniol.

exposure ($P < 0.001$ for all). The expression of caspase 9 was similar between two doses of Ge in CP exposure ($P > 0.05$). The mean intensity of expression was 25.07 ± 0.89 in CP+Ge 100 group, while it was 25.43 ± 0.98 in CP+Ge 200 group. The expression level of caspase 3 was significantly enhanced at a dosage of

200 mg/kg (23.21 ± 1.86) in comparison to 100 mg/kg (25.46 ± 1.03) ($P = 0.006$) (Table 1). Figure 3 and Figure 4 illustrate the immunofluorescence labeling of caspase 3 and caspase 9 expressions, together with the mean intensity values across the groups, respectively.

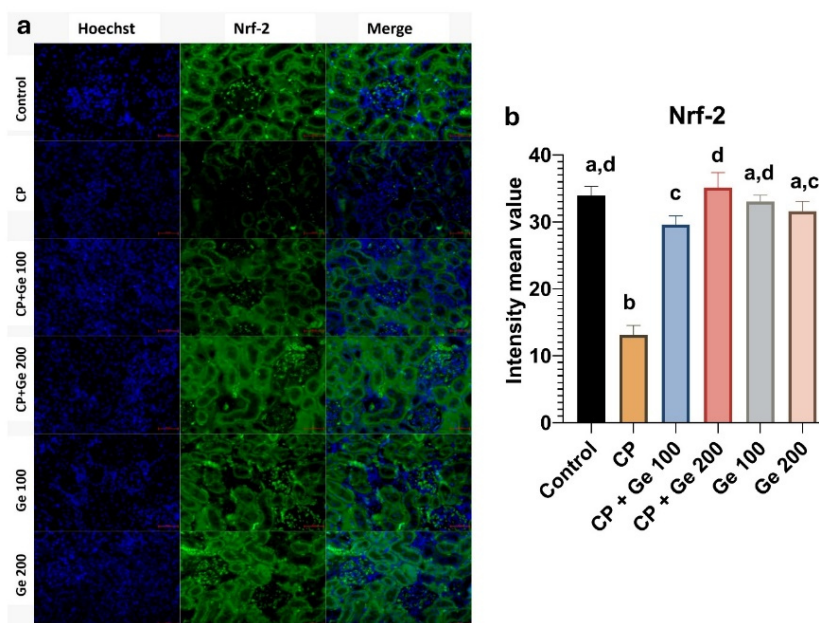


FIGURE 3. (a) Immunofluorescence staining of Nrf-2 among the groups. Bars show 50 μm (×200). (b) Nrf-2 intensity mean values of the experimental groups. There is statistically significant difference between the groups not sharing the same letter ($P < 0.05$). CP, Cyclophosphamide; Ge, Geraniol; Nrf-2, nuclear factor erythroid 2-related factor 2.

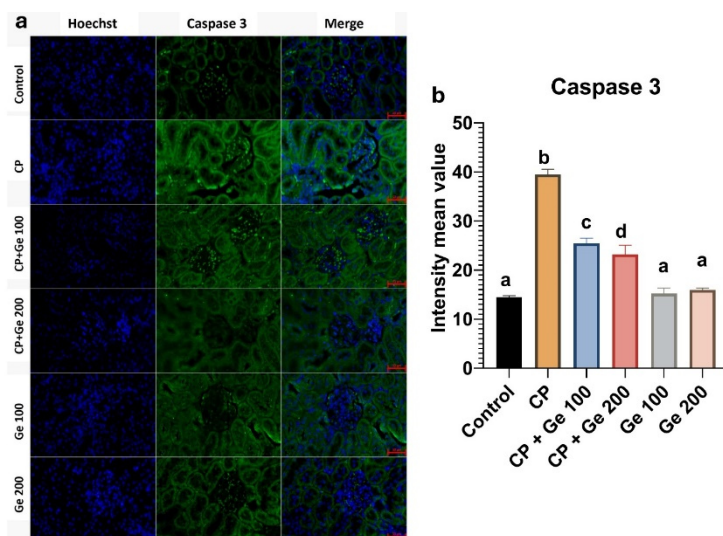


FIGURE 4. (a) Immunofluorescence staining of caspase 3 among the groups. Bars show 50 μm (×200). (b) caspase 3 intensity mean values of the experimental groups. There is statistically significant difference between the groups not sharing the same letter (P<0.05). CP, Cyclophosphamide; Ge, Geraniol.

DISCUSSION

This study demonstrated that nephrotoxicity occurred in rats administered CP. GE administration was determined to rectify this damage in a dose-dependent way. This effect was found to be associated with changes in the Nrf-2 pathway and caspase 3 and caspase 9 levels in an antiapoptotic direction.

This study demonstrated that CP administration

caused renal damage based on histopathological assessment. Tubular degeneration and dilation, vacuolization, impaired renal architecture, inflammatory infiltration, and fibrotic changes were observed. These findings align with previous studies that established a model of nephrotoxicity associated with chemotherapeutic agents [14, 15]. However, a significant improvement in histopathological findings was observed with Ge administration. Several

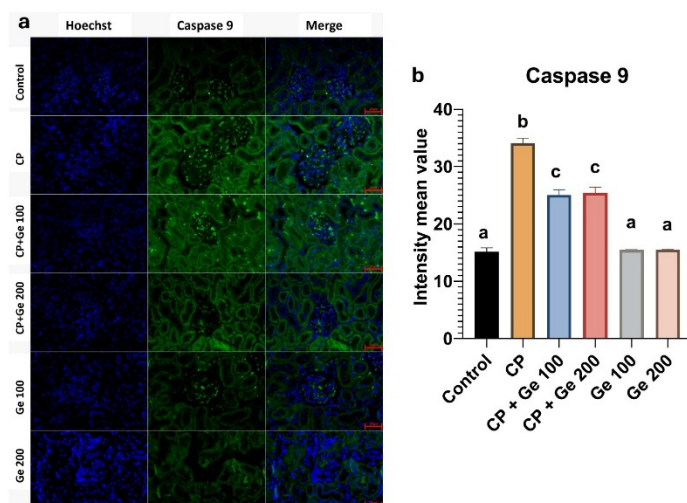


FIGURE 5. (a) Immunofluorescence staining of caspase 9 among the groups. Bars show 50 μm (×200). (b) caspase 9 intensity mean values of the experimental groups. There is statistically significant difference between the groups not sharing the same letter (P<0.05). CP, Cyclophosphamide; Ge, Geraniol.

compounds and antioxidants have improved renal structure against the nephrotoxicity in the current literature [16, 17]. The maintenance of tubular integrity and the reversal of degenerative alterations underscore the protective properties of Ge. Ge has a dose-dependent effect; as its nephroprotective activity is more prominent in higher dose. Our findings altogether demonstrate that Ge significantly alleviates renal injury induced by CP.

In our study, immunofluorescence assessment indicated that CP treatment decreased Nrf-2 expression. This finding supports the idea that oxidative stress plays a significant role in the development of CP-induced nephrotoxicity, given that Nrf-2 is a principal regulator of cellular antioxidant defense mechanism. Previous studies have also demonstrated that oxidative stress and the Nrf-2 pathway play a crucial role in the development of nephrotoxicity associated with chemotherapy agents [8, 18].

A significant increase in Nrf-2 expression was observed following Ge treatment in the present study. The activation of Nrf-2 induces an antioxidant response in cells [5]. Antioxidants have been found to effectively reverse kidney damage caused by CP-induced nephrotoxicity via the Nrf-2 pathway [4, 19]. Consequently, our data indicates that Ge may effectively mitigate oxidative damage in renal tissue through a Nrf-2-mediated mechanism. While the downstream targets of Nrf-2 were not assessed in this investigation, the noted expression alterations serve as a substantial signal of the activation of the antioxidant defense system.

Apoptosis is a crucial mechanism in nephrotoxicity induced by anticancer treatment. The elevation of caspase 3 and caspase 9 expression by CP in our study corroborates this mechanism and aligns with existing literature [20, 21]. The observed anti-apoptotic changes, especially at high doses, with the Ge application are consistent with histological findings. This study demonstrates that Ge can modulate not only oxidative stress but also apoptosis. Oxidative stress is acknowledged to initiate apoptotic pathways [22, 23]. Caspase enzymes are important to this process [24, 25]. This study indicates that the elevation of Nrf-2 and the reduction of caspase 3 and caspase 9 levels in an anti-apoptotic manner imply that Ge's mode of action is complex. Ge provides

nephroprotection by modulating the cellular stress response and apoptotic processes.

An important finding of this study is that the effect of Ge is dose-dependent. Both histological and immunofluorescence assessments including Nrf-2 and caspase 3 indicate that Ge exhibits greater efficacy at higher dose. The dose-response relationship is important in demonstrating the reliability of the findings and the therapeutic efficacy of Ge.

Ge, a natural compound, may serve as an adjunctive strategy to mitigate CP-induced renal damage in clinical settings. Nevertheless, further molecular and clinical investigations are needed to confirm its translational applicability.

Strengths and Limitations

This investigation possesses several limitations. Initially, oxidative stress indicators could not be quantified biochemically. Likewise, renal function tests, including serum creatinine and blood urea nitrogen levels, were not assessed. Furthermore, extensive molecular investigations, such as Western blotting and PCR, were not conducted. The inability to assess Nrf-2 downstream targets constrains the capacity to derive mechanistic conclusions. Nonetheless, corroboration of histological findings using immunofluorescence assessments enhances the confidence of the outcomes. An additional strength of this study is the evaluation of two different Ge doses, which allowed assessment of a potential dose-dependent response, while the concurrent evaluation of Nrf-2, caspase-3, and caspase-9 provided insight into both antioxidant and apoptosis-related processes associated with CP-induced nephrotoxicity.

CONCLUSION

Histopathological findings of this study demonstrated that CP induces renal damage and Ge seems to be effective in reversing this damage. Ge may achieve renal recovery by activating antioxidant and antiapoptotic pathways. Ge may represent a promising effect at both doses; however, its efficacy is more pronounced at the higher dose.

Ethics Approval and Consent to Participate

This study was approved by the Necmettin

Erbakan University KONÜDAM Experimental Medicine Application and Research Center Animal Experiments Local Ethics Committee (Decision No: 2017/039; date: 22.12.2017). All experimental procedures involving animals were conducted in accordance with the ethical standards of the Guide for the Care and Use of Laboratory Animals published by the U.S. National Institutes of Health and Institutional authority. All efforts were made to minimize animal suffering and to reduce the number of animals used.

Clinical Trial Registration
Not Available.

Data Availability

All data generated or analyzed during this study are included in this published article. The data that support the findings of this study are available on request from the corresponding author, upon reasonable request.

Authors' Contribution

Study Conception: HTC, MES, FAC, GC, SK; Study Design: HTC, MES, FAC, GC, SK; Supervision: HTC, MES, FAC, GC, SK; Funding: HTC, MES; Materials: N/A; Data Collection and/or Processing: HTC, MES; Statistical Analysis and/or Data Interpretation: HTC, FAC; Literature Review: HTC, FAC; Manuscript Preparation: HTC; and Critical Review: GC, SK.

Conflict of Interest

The author(s) disclosed no conflict of interest during the preparation or publication of this manuscript.

Financing

The author(s) disclosed that they did not receive any grant during the conduct or writing of this study.

Acknowledgments

The authors have no acknowledgments to declare.

Generative Artificial Intelligence Statement

The author(s) declare that no artificial intelligence-based tools or applications were used during the preparation process of this manuscript. The all content of the study was produced by the author(s) in accordance with scientific research methods and academic ethical principles.

Editor's Note

All statements made in this article are solely those of the authors and do not represent the views of their affiliates or the publisher, editors, or reviewers. Any claims made by any product or manufacturer that may be evaluated in this article are not guaranteed or endorsed by the publisher.

REFERENCES

1. Ayza MA, Zewdie KA, Yigzaw EF, et al. Potential Protective Effects of Antioxidants against Cyclophosphamide-Induced Nephrotoxicity. *Int J Nephrol.* 2022;2022:5096825. doi: [10.1155/2022/5096825](https://doi.org/10.1155/2022/5096825).
2. Oberiukhtin D, Chernitskiy A, Hu D, Sarapultsev A. Cyclophosphamide-Induced Nephrotoxicity and Nephroprotection in Rodent Models: A Systematic Review and Random-Effects Meta-Analysis (2010–2025). *J Xenobiotics.* 2026;16(2):48. doi: [10.3390/jox16020048](https://doi.org/10.3390/jox16020048).
3. Wu Q, Wang X, Nepovimova E, Wang Y, Yang H, Kuca K. Mechanism of cyclosporine A nephrotoxicity: Oxidative stress, autophagy, and signalings. *Food Chem Toxicol.* 2018;118:889–907. doi: [10.1016/j.fct.2018.06.054](https://doi.org/10.1016/j.fct.2018.06.054).
4. Ranasinghe R, Mathai M, Zulli A. Cytoprotective remedies for ameliorating nephrotoxicity induced by renal oxidative stress. *Life Sci.* 2023;318:121466. doi: [10.1016/j.lfs.2023.121466](https://doi.org/10.1016/j.lfs.2023.121466).
5. Dong W, Wan J, Yu H, et al. Nrf2 protects against methamphetamine-induced nephrotoxicity by mitigating oxidative stress and autophagy in mice. *Toxicol Lett.* 2023;384:136–148. doi: [10.1016/j.toxlet.2023.08.002](https://doi.org/10.1016/j.toxlet.2023.08.002).
6. Caglayan C, Temel Y, Kandemir FM, Yildirim S, Kucukler S. Naringin protects against cyclophosphamide-induced hepatotoxicity and nephrotoxicity through modulation of oxidative stress, inflammation, apoptosis, autophagy, and DNA damage. *Environ Sci Pollut Res.* 2018;25(21):20968–20984. doi: [10.1007/s11356-018-2242-5](https://doi.org/10.1007/s11356-018-2242-5).
7. Ijaz MU, Mustafa S, Batool R, Naz H, Ahmed H, Anwar H. Ameliorative effect of herbacetin against cyclophosphamide-induced nephrotoxicity in rats via attenuation of oxidative stress, inflammation, apoptosis and mitochondrial dysfunction. *Hum Exp Toxicol.* 2022;41:9603271221132140. doi: [10.1177/09603271221132140](https://doi.org/10.1177/09603271221132140).
8. Alasmari AF, Ali N, Alharbi M, et al. Geraniol Ameliorates Doxorubicin-Mediated Kidney Injury through Alteration of Antioxidant Status, Inflammation, and Apoptosis: Potential Roles of NF-κB and Nrf2/Ho-1. *Nutrients.* 2022;14(8):1620. doi: [10.3390/NU14081620](https://doi.org/10.3390/NU14081620).
9. Mahmoud NM, Elshazly SM, Rezaq S. Geraniol protects against cyclosporine A-induced renal injury in rats: Role of Wnt/β-catenin and PPARγ signaling pathways. *Life Sci.* 2022;291:120259. doi: [10.1016/j.lfs.2021.120259](https://doi.org/10.1016/j.lfs.2021.120259).
10. Cuce G, Esen HH, Koc T, et al. Vitamin E partially ameliorates cyclophosphamide-induced nephrotoxicity in rats. *Prog Nutr.* 2016;18(2):140–145.
11. Mohamed ME, Elmorsy MA, Younis NS. Renal

- Ischemia/Reperfusion Mitigation via Geraniol: The Role of Nrf-2/HO-1/NQO-1 and TLR2,4/MYD88/NFκB Pathway. *Antioxidants* (Basel). 2022;11(8):1568. doi: 10.3390/antiox11081568.
12. Canbaz HT, Sozen ME, Cinar Ayan I, et al. Effects of Carvacrol on Oxidative Stress and Fibrosis in Streptozotocin-Induced Diabetic Nephropathy: Histological, Gene Expression, and Biochemical Insights. *Int J Mol Sci*. 2025;27(1):291. doi: 10.3390/ijms27010291.
13. Gültekin B, Çetinkaya Karabekir S, Çinar Ayan İ, Basri Savaş H, Kalkan S. Protective role of astaxanthin against bisphenol A induced biochemical and histopathological alterations in rat kidneys. *Iran J Basic Med Sci*. 2025;28(12):1647–1655. doi: 10.22038/ijbms.2025.88356.19081.
14. Mombeini MA, Kalantar H, Sadeghi E, Goudarzi M, Khalili H, Kalantar M. Protective effects of berberine as a natural antioxidant and anti-inflammatory agent against nephrotoxicity induced by cyclophosphamide in mice. *Naunyn Schmiedebergs Arch Pharmacol*. 2022;395(2):187–194. doi: 10.1007/s00210-021-02182-3.
15. Wanas H, El-Shabrawy M, Mishriki A, Attia H, Emam M, Aboulhoda BE. Nebivolol protects against cyclophosphamide-induced nephrotoxicity through modulation of oxidative stress, inflammation, and apoptosis. *Clin Exp Pharmacol Physiol*. 2021;48(5):811–819. doi: 10.1111/1440-1681.13481.
16. Salama RM, Nasr MM, Abdelhakeem JI, Roshdy OK, ElGamal MA. Alogliptin attenuates cyclophosphamide-induced nephrotoxicity: a novel therapeutic approach through modulating MAP3K/JNK/SMAD3 signaling cascade. *Drug Chem Toxicol*. 2022;45(3):1254–1263. doi: 10.1080/01480545.2020.1814319.
17. Temel Y, Kucukler S, Yildirim S, Caglayan C, Kandemir FM. Protective effect of chrysin on cyclophosphamide-induced hepatotoxicity and nephrotoxicity via the inhibition of oxidative stress, inflammation, and apoptosis. *Naunyn Schmiedebergs Arch Pharmacol*. 2020;393(3):325–337. doi: 10.1007/s00210-019-01741-z.
18. Dil E, Topcu A, Mercantepe T, et al. Agomelatine on cisplatin-induced nephrotoxicity via oxidative stress and apoptosis. *Naunyn Schmiedebergs Arch Pharmacol*. 2023;396(10):2753–2764. doi: 10.1007/s00210-023-02632-0.
19. Uyumlu AB, Satılmış B, Atıcı B, Taşlıdere A. Phenethyl isothiocyanate protects against cyclophosphamide-induced nephrotoxicity via nuclear factor E2-related factor 2 pathway in rats. *Exp Biol Med* (Maywood). 2023;248(2):157–164. doi: 10.1177/15353702221139206.
20. Sinanoglu O, Yener AN, Ekici S, Midi A, Aksungar FB. The protective effects of spirulina in cyclophosphamide induced nephrotoxicity and urotoxicity in rats. *Urology*. 2012;80(6):1392.e1-1392.e6. doi: 10.1016/j.urology.2012.06.053.
21. Fouad AA, Qutub HO, Al-Melhim WN. Punicalagin alleviates hepatotoxicity in rats challenged with cyclophosphamide. *Environ Toxicol Pharmacol*. 2016;45:158–162. doi: 10.1016/j.etap.2016.05.031.
22. Sozen ME, Savas HB, Cuce G. Protective Effects of Selenium against Acrylamide-Induced Hepatotoxicity in Rats. *Pak Vet J*. 2024;44(2):274–279. doi: 10.29261/pakvetj/2024.153.
23. Kannan K, Jain SK. Oxidative stress and apoptosis. *Pathophysiology*. 2000;7(3):153–163. doi: 10.1016/s0928-4680(00)00053-5.
24. Karabekir SC, Sozen ME, Ayan IC, Savas HB, Cuce G, Kalkan S. The ameliorative effects of hesperidin in rats developed hepatotoxicity with deltamethrin. *Iran J Basic Med Sci*. 2025;28(7):929–936. doi: 10.22038/ijbms.2025.82598.17854.
25. Asadi M, Taghizadeh S, Kaviani E, et al. Caspase-3: Structure, function, and biotechnological aspects. *Biotechnol Appl Biochem*. 2022;69(4):1633–1645. doi: 10.1002/bab.2233.